 doi:10.20944/preprints202011.0580.v1

Article

Optimization of the Mix Formulation of Geopolymer using Nickel-laterite Mine Waste and Coal Fly Ash

Alberto Longos Jr [1,*], April Anne Tigue [1], Ithan Jessemar Dollente [1], Roy Alvin Malenab [1], Ivyleen Bernardo-Arugay [2], Hirofumi Hinode [3], Winarto Kurniawan [3] and Michael Angelo Promentilla [1,*]

[1] Chemical Engineering Department, De La Salle University-Manila; alberto_longos@dlsu.edu.ph (A.L.); april_tigue@dlsu.edu.ph (A.T.); roy.malenab@dlsu.edu.ph (R.M.); ithan_dollente@dlsu.edu.ph (I.D.)
2 Materials and Resources Engineering and Technology, MSU-Iligan Institute of Technology; ivyleen.arugay@g.msuiit.edu.ph (I.A.)
3 Department of Transdisciplinary Science and Engineering, Tokyo Institute of Technology, Tokyo, Japan; hinode.h.aa@m.titech.ac.jp (H.H.); kurniawan.w.ab@m.titech.ac.jp (W.K.)
* Correspondence: michael.promentilla@dlsu.edu.ph (M.P.); alberto_longos@dlsu.edu.ph (A.L.); +63-917-545-2243 (M.P.) ; +63-917-316-4005 (A.L.)

Abstract: Geopolymer cement has been popularly studied nowadays compared to ordinary Portland cement but has demonstrated superior environmental advantages due to its lower carbon emissions and waste material utilization. Several studies on geopolymers have utilized various wastes like fly ash, blast furnace slag, silica fume, rice husk, or a combination of these wastes. This paper presents a mix formulation design experiment to produce a geopolymer from nickel-laterite mine waste (NMW) and coal fly ash (CFA) as a geopolymer precursor, and sodium hydroxide (SH) and sodium silicate (SS) as alkali activators. An I-optimal design experiment is used to predict the compressive strength for all the mixture's possible formulations and identify optimal proportions to minimize the average variance of prediction. A mixed formulation run of 50% NMW, SH-to-SS ratio of 0.5, and an activator-to-precursor ratio of 0.4286 yielded the highest 28-day unconfined compressive strength (UCS) of 22.1±5.4 MPa. Furthermore, using an optimized formulation of 50.12% NMW, SH-to-SS ratio of 0.516, and an activator-to-precursor ratio of 0.428, an actual UCS value of 36.26±3.6 MPa was obtained. The result implies that the synthesized geopolymer material can be potentially used for pedestrian pavers, light traffic pavers, plain concrete for leveling, building bricks, ceramic glazed facing brick, and fired clay bricks.

Keywords: geopolymer; laterite; alkali-activated; alumino-silicates; I-optimal; response surface methodology; optimization; mine waste

1. Introduction

The rapid increase in construction activity has been observed to meet the ever-increasing infrastructure demands [1]. In most construction activities, cement-based concrete is an essential and very widely used material. The use of cement-based concrete, like ordinary Portland cement (OPC), is globally accepted due to ease of operation, mechanical properties, and low-cost production compared to other construction materials [2]. However, there are drawbacks of OPC like it releases approximately one ton of CO_2, a greenhouse gas, to produce one ton of OPC [3], high energy consumption during production [4], and consumes a significant amount of natural resources [2]. Due to increasing awareness of this issue, a viable alternative for the conventional Portland cement is currently being reviewed and studied by many researchers and scientists. Geopolymer cement is one of the emerging greener alternatives for the construction industry. It is usually the result of the chemical reaction between aluminosilicate waste materials and alkaline activators [4]. It is comprised of repeating units of silico-oxide (Si–O–Si), silico-aluminate (Si–O–Al–O-), Ferro-silico-aluminate (-Fe-O-Si-O-Al-O-), or alumino-phosphate (-Al-O-P-O-), created through a process of

Preprints (www.preprints.org) | NOT PEER-REVIEWED | Posted: 23 November 2020 doi:10.20944/preprints202011.0580.v1

geopolymerization [5]. Aluminosilicate waste material sources, also called a geopolymer precursor, can be from fly ash, blast furnace slag, silica fume, and rice husk or a combination of these precursors, which are rich from silicon (Si), aluminum (Al), or iron (Fe) in an amorphous form [6]. Mine wastes from nickel-laterite mine have also been starting to emerge and explore as a geopolymer precursor because it contains Si, Al, and Fe and at the same time can address the waste it generated at about 136,000 m^3/yr [7]. It has also been studied that this mine waste is a potential geopolymer precursor which enhances its cementitious activity after thermal and mechanical activations as product pretreatment[7]. There are studies that geopolymer precursors are combined, like fly ash and granulated blast furnace, and determined the optimal rational mix design [1] resulted in a compressive strength comparable to OPC ranging from 32 to 66 MPa. In another study of [8], it was reported that addition of fly ash to mine tailings (MT) resulted in a higher compressive strength than MT-based geopolymer and can be viable and promising construction material which can be tailored for different applications.

Thus, this study aims to determine the mix formulation of coal fly ash (CFA) and nickel-laterite mine waste (NMW) as geopolymer precursors with sodium hydroxide (SH)-sodium silicate (SS) mixture as alkali activators to obtain an optimum compressive strength of the produced geopolymer. Optimum parameters used were in terms of %NMW (in NMW-CFA content), precursor-to-activator ratio, and SH-to-SS ratio.

2. Materials and Methods

2.1. Raw Material Preparation and Characterization

Raw NMW was collected from a siltation pond of a nickel-laterite mining company while CFA was obtained from a coal power plant located in Mindanao. Raw materials were oven-dried at 105 ^oC for 24 hours. Dried NMW showed clay-like characteristics, and the clumping of this clayey material facilitated the need for pre-grinding. The dried NMW was reduced in size using a pulverizer. On the other hand, dried CFA already exhibited the needed fineness and will have no need for further grinding. Both raw material samples were then screened using a Tyler mesh sieve passing 50 mesh (297 μm). Analytical grade of sodium silicate with 34.13% SiO_2, 14.65% Na_2O and sodium hydroxide with 99% purity were used in the study as the alkali activator components. The chemical compositions of raw NMW and CFA were performed using X-ray fluorescence spectroscopy and are reported in Table 1.

Table 1. Chemical Composition of raw NMW and CFA.

Mass %	SiO_2	Al_2O_3	Fe_2O_3	CaO	MgO	NiO	Others	LOI
Raw NMW	24.31	3.30	56.43	6.46	5.00	2.29	2.21	15.50
Coal Fly ash	27.21	8.34	23.65	30.57	2.06	0.03	2.61	0

Toxicity characteristics leaching procedure (TCLP) using US EPA Method 1311 was also performed for both raw materials to determine the heavy metal leachability property whether these materials are hazardous or not and is reported to be non-hazardous in Table 2. Samples were then analyzed using an inductively coupled plasma- mass spectrometry (ICP-MS) and inductively coupled plasma- optical emission spectroscopy (ICP-OES).

Table 2. TCLP Analysis of Raw Materials Samples in mg/L.

	Ag	As	Ba	Cd	Cr	Hg	Pb	Se
TCLP Limit	5.0	5.0	100.0	1.0	5.0	0.2	5.0	1.0
CFA	0.00051	0.069225	2.54405	0.000425	0.035	0.00085	0.0027	0.02285
Raw NMW	0.000455	0.00005	0.10854	0.00037	0.19	0.0001	0.00335	0.001

The mineralogical analysis was also performed for both raw materials using an X-ray Diffractometer (XRD), and its pattern is shown in Figure 1. It was observed that raw NMW

Preprints (www.preprints.org) | NOT PEER-REVIEWED | Posted: 23 November 2020 doi:10.20944/preprints202011.0580.v1

dominantly contains minerals such as kaolinite or dickite ($Al_2Si_2O_5(OH)_4$), montmorillonite ($(Na,Ca)_{0.3}(Al,Mg)_2Si_4O_{10}(OH)_2 \cdot nH_2O$), quartz ($SiO_2$), and hematite ($Fe_2O_3$). On the second and fifth peak of the XRD pattern, either a kaolinite or dickite is observed which both minerals belong to the same kaolin family. However, it is observed based from XRD library of both minerals that dickite is more prevalent than kaolinite. On the other hand, CFA contains minerals such as quartz (SiO_2) and hematite (Fe_2O_3). A hump background between 19°-23°, 33°-37° 2θ for raw NMW, and between 26°-27°, 35°-37° 2θ for CFA may correspond to the amorphous content of the material. It is believed that the amorphous content of the material has played a significant role in geopolymerization due to its reactive nature. This inference can be correlated with the study conducted by [9] wherein materials having high amorphous content were found to yield a geopolymer having a better mechanical property in binders.

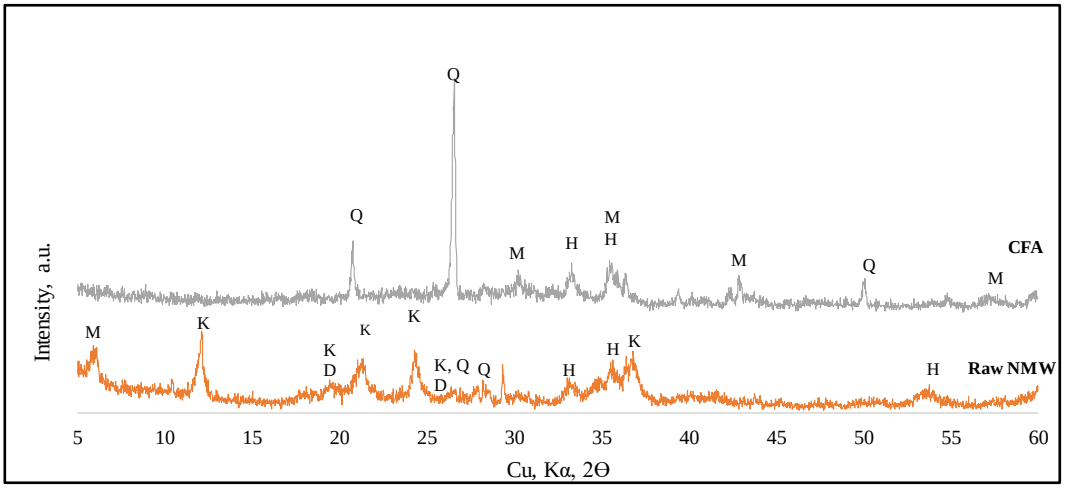

Figure 1. Mineralogical pattern of raw materials (M-montmorillonite; K-kaolinite; D-dickite; Q-quartz; H-hematite).

SEM images of raw materials were also captured, as shown in Figure 2. The structure of the raw nickel laterite mine waste is platy and loose with sheets, which is favorable for water storage [10]. On the other hand, coal fly ash images show that most of the particles are spherical (cenosphere) or are occurring as microspheres and are more loose than the NMW particles. These microspheres increase the specific surface area of the fly ash [11]. Thus, there is a high probability that the total surface are of CFA is higher than coarser platy structure of NMW which might make the CFA to be more reactive than NMW.

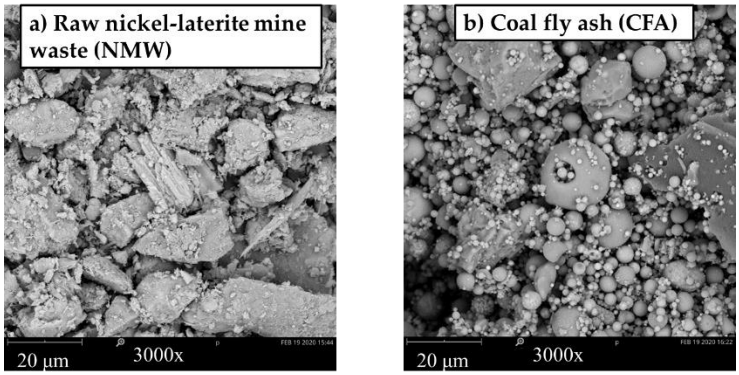

Figure 2. SEM Images at magnification 3000x for (a) raw nickel-laterite mine waste and (b) coal fly ash.

2.2. Thermal Activation of Nickel-laterite Mine Waste (NMW)

Preprints (www.preprints.org) | NOT PEER-REVIEWED | Posted: 23 November 2020 doi:10.20944/preprints202011.0580.v1

Pre-treatment of NMW by thermal activation was performed first before experimental runs were conducted. This step is based on the study of [7] that thermal activation enhances the cementitious activity of the NMW for geopolymer synthesis. NMW samples were heat treated in the laboratory furnace at a ramping rate of 10 °C per minute to attain a temperature of 700 °C at a holding time of two hours. The samples were left inside the furnace to be cooled down to room temperature after soaking at 700 °C.

2.3. Experimental Procedures and Runs

The design of the experiment was based on an I-optimal design, which is a mixture experiment intended to predict the responses for all possible formulations of the mixture and to identify optimal proportions for each of the ingredients minimizing the average variance of prediction. The factors and levels selection were based on various references related to the study [12], [13], [14], [8], [15], [16]. Table 3 shows the factors used in the mixture design, and the performance of the different factors was evaluated independently using runs randomly ordered by Design Expert 11 software (Design-Expert® software, version 11). A total of 18 runs were generated with three as replicate points. The 18 experimental runs are shown in Table 4 with different combinations of factor levels.

Table 3. Parameters of each factor and level for geopolymer synthesis.

Factors	Low Level	Mid Level	High Level
1. Activator-to-Precursor ratio	-1 (0.4286)	0 (0.6667)	1 (1)
2. NMW-CFA content, as % NMW	-1 (50%)	0 (75%)	1 (100%)
3. SH-to-SS ratio	-1 (1:2)	(0 (1:1)	1 (2:1)

Table 4. Experimental runs in standard order.

Std order	Run order	Factor 1: Activator-to-Precursor ratio	Factor 2: NMW-CFA content as % NMW	Factor 3: SH-to-SS ratio
1	15	0.4286	50%	1:2
2	5	1.0000	50%	1:2
3	6	0.4286	75%	1:2
4	10	0.6667	100%	1:2
5	16	1.0000	100%	1:2
6	9	0.6667	50%	1:1
7	1	0.6667	50%	1:1
8	2	0.6667	75%	1:1
9	11	0.6667	75%	1:1
10	8	0.6667	75%	1:1
11	4	1.0000	75%	1:1
12	12	0.4286	100%	1:1
13	3	0.4286	50%	2:1
14	7	1.0000	50%	2:1
15	18	0.6667	75%	2:1
16	17	1.0000	75%	2:1
17	14	0.4286	100%	2:1
18	13	1.0000	100%	2:1

Preprints (www.preprints.org) | NOT PEER-REVIEWED | Posted: 23 November 2020 doi:10.20944/preprints202011.0580.v1

2.4. Geopolymer Synthesis

For the preparation of geopolymer, run number 15 will be the basis of the amounts of raw materials used. A 500 g of precursor (50% NMW+CFA) was prepared and set aside first for mixing later. With an activator-to-precursor of 0.438, the alkali activator was prepared first by mixing 71 g of 12 M sodium hydroxide (SH) with 143 g sodium silicate (SS). Then, 250 g of CFA was mixed with the prepared alkali activator. Manual mixing was done for at least 5 minutes until the consistency of the CFA-activator mixture was homogenized. Another 250 g of NMW was then added to the mixture and a second stage of manual mixing was done for at least 5 minutes until the consistency of the mixture was again homogenized. During mixing, it must be noted that the mixture hardens immediately. After stabilization, the geopolymer was placed in a square mold made of polyethylene material with a dimension 50 mm x 50 mm x 50 mm. The prepared geopolymer can make 3 square molds. The molded sample was set for at least 24 hours before it was demolded. The demolded sample was then placed in a polyethylene ziplock. Air was removed manually and sealed. It was then placed in an oven at 80 ^{o}C for 24 hours. The sealed geopolymer sample was cured for 28 days at ambient temperature before further test and analysis.

2.5. Unconfined Compressive Strength (UCS)

Unconfined compressive strength (UCS) was the response variable and the determining engineering property for evaluation. It was performed following ASTM C109/C109M. This test method covers the determination of the compressive strength of hydraulic cement mortars, using 2-in. or [50-mm] cube specimens to determine compliance with specifications. Further, this test method is referenced by numerous other specifications and test methods. Caution must be exercised in using the results of this test method to predict the strength of concretes.

3. Results and Discussions

3.1. Statistical Analysis

3.1.1. Unconfined Compressive Strength (UCS)

The unconfined compressive strengths of the synthesized geopolymer were observed to range from 1.93 MPa up to 22.14 MPa after 28 days, as shown in Figure 3. The experimental formulation mix number 15 with an activator-to-precursor ratio of 0.4286, 50% NMW, and with SH-to-SS ratio of 1:2 yields the highest value making it the best mix sample among other runs. The sample with an activator-to-precursor ratio of 1, 100% NMW with 2 parts of sodium hydroxide and 1 part sodium silicate (SH-to-SS ratio of 2:1) resulted into deflocculation of NMW, hence it did not harden. This may be because of the combination of factors such as the precursor is 100% NMW which is not that reactive. Moreover, this may also be because the ratio of SH-to-SS is high which means 12 M NaOH has large amount which further lowers the overall concentration of SiO_3 and Al_2O_3 affecting its participation to the reaction.

This observation may have been due to the combination of the following factors: (1) The precursor is 100% NMW, which is not that reactive, (2) The activator-to-precursor of 1, which means that the mixture has more activator in liquid form and may have been excess in the reaction, and (3) the ratio of SH-to-SS is high, which means that the 12 M NaOH has overpowered the activator, lowering the overall concentration of SiO_3 and Al_2O_3, and thus affecting the geopolymerization.

Preprints (www.preprints.org) | NOT PEER-REVIEWED | Posted: 23 November 2020 doi:10.20944/preprints202011.0580.v1

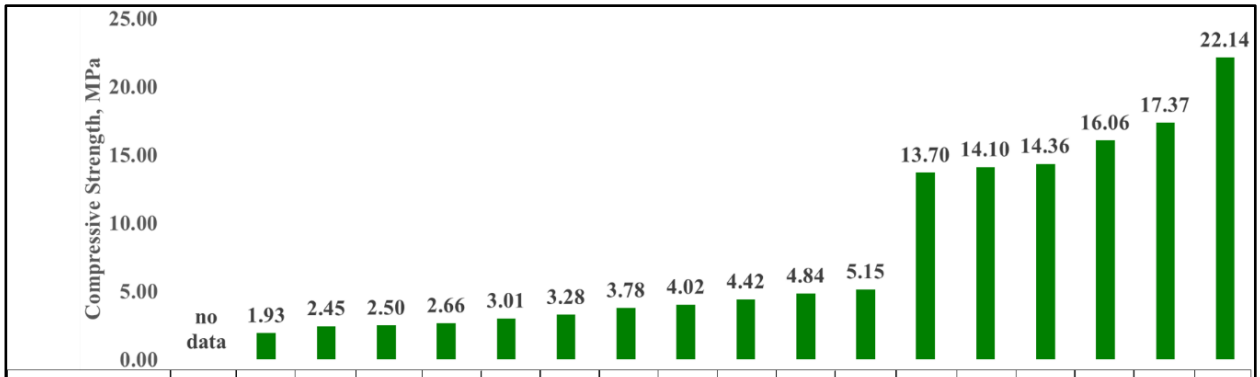

Run Order	13	17	4	7	18	14	16	12	8	10	11	2	6	3	5	9	1	15
Factor 1: Activator: Precursor ratio	1.00	1.00	1.00	1.00	0.667	0.429	1.00	0.429	0.667	0.667	0.667	0.667	0.429	0.429	1.00	0.667	0.667	0.429
Factor 2: NMW-CFA content % NMW	100	75	75	50	75	100	100	100	75	100	75	75	75	50	50	50	50	50
Factor 3: SH-to-SS ratio	2:1	2:1	1:1	2:1	2:1	2:1	1:2	1:1	1:1	1:2	1:1	1:1	1:2	2:1	1:2	1:1	1:1	1:2

Figure 3. Comparison of unconfined compressive strength at different mix proportions.

3.1.2. Model Statistics

The summary of model statistics suggested that the model used must be the maximized adjusted R-squared and predicted R-squared and the model must also be not aliased which for Table 5, the suggested model for analysis is quadratic with an adjusted R-squared of 92.69% and predicted R-squared of 80.97%

Table 5. Summary of model statistics for UCS.

Source	Std. Dev.	R^2	Adjusted R^2	Predicted R^2	
Linear	3.10	0.8232	0.7853	0.7036	
2FI	2.64	0.8989	0.8438	0.7483	
Quadratic	**1.81**	**0.9656**	**0.9269**	**0.8097**	**Suggested**
Cubic	0.7164	0.9980	0.9885		Aliased

The quadratic model as can be shown in Table 6 indicates that the model is significant. P-values less than 0.0500 indicate model terms are significant. In this case A, B, C, AB, BC, B^2 are significant model terms. Since AC, A^2 and C^2 have insignificant p-values, the model is reduced and the new ANOVA with reduced quadratic model is shown in Table 7.

3.1.2. Analysis of Variance (ANOVA)

Analysis of Variance (ANOVA) indicates that all three (3) factors significantly affect the compressive strength of the synthesized geopolymer (Table 7). The relationship of individual factors with its compressive strength is shown in Figure 4. In terms of activator-to-precursor ratio (A), it can be observed that the compressive strength of the synthesized geopolymer increases as the activator-to-precursor ratio decreases. This result may have been because more precursor is present in the system to participate in the geopolymerization process. On the other hand, the compressive strength of the synthesized geopolymer increases when the percentage of NMW (B) decreases quadratically. This observation may be due to the increase in coal fly ash percentage, which is more reactive than the NMW. Moreover, compressive strength also increases when the SH-to-SS ratio (C) decreases. The decrease of the said ratio means more SS in the solution, which means more SiO_3 content in the system can participate in the geopolymerization reaction.

Preprints (www.preprints.org) | NOT PEER-REVIEWED | Posted: 23 November 2020 doi:10.20944/preprints202011.0580.v1

Table 6. ANOVA for the Quadratic Model.

Source	Sum of Squares	df	Mean Square	F-value	p-value	
Model	**735.05**	**9**	**81.67**	**24.94**	**<0.0001**	**significant**
A-Activator-to-Precursor ratio	99.69	1	99.69	30.44	0.0006	significant
B-NMW-CFA Content	320.70	1	320.70	97.93	<0.0001	significant
C-SH-to-SS ratio	107.22	1	107.22	32.74	0.0004	significant
AB	24.69	1	24.69	7.54	0.0252	significant
AC	0.02	1	0.02	0.01	0.9451	not significant
BC	27.62	1	27.62	8.43	0.0198	significant
A^2	0.45	1	0.45	0.14	0.7200	not significant
B^2	25.45	1	25.45	7.77	0.0236	significant
C^2	4.22	1	4.22	1.29	0.2890	not significant
Residual	**26.20**	**8**	**3.27**			
Lack of Fit	24.66	5	4.93	9.61	0.0458	significant
Pure Error	1.54	3	0.51			
Cor Total	761.25	17				

Table 7. ANOVA for the Reduced Quadratic Model.

Source	Sum of Squares	df	Mean Square	F-value	p-value	
Model	727.58	6	121.26	39.61	< 0.0001	significant
A-Activator-to-Precursor ratio	95.31	1	95.31	31.13	0.0002	
B-NMW-CFA Content (%NMW)	315.15	1	315.15	102.94	< 0.0001	
C-SH-to-SS ratio	100.18	1	100.18	32.72	0.0001	
AB	29.33	1	29.33	9.58	0.0102	
BC	28.54	1	28.54	9.32	0.0110	
B^2	44.58	1	44.58	14.56	0.0029	
Residual	33.68	11	3.06			not significant
Lack of Fit	32.14	8	4.02	7.83	0.0591	
Pure Error	1.54	3	0.5133			
Cor Total	761.25					

Figure 5 shows the interaction graph of AB and BC. The interaction of factors A (activator-to-precursor ratio) and B (% NMW) shows that the compressive strength increases as both factors decrease (Figure 5a). Decreasing the % NMW (B) corresponds to the increase of CFA content in the system, in which CFA is more reactive for geopolymerization. Moreover, when the activator-to-precursor ratio (A) decreases, a higher precursor amount is present in the system. When the amount of precursor is increased, the geopolymerization reaction is boosted because of the high reactivity of CFA - increasing the compressive strength of the product.

Similarly, Figure 5b also shows the interaction of factors B (% NMW) and C (SH-to-SS ratio) that compressive strength also increases as both factors B and C decreases. The possible explanation for this is that when % NMW is decreased, more CFA is present in the system. Moreover, when SH-to-SS is decreased, it means a high value of SS (Na_2SiO_3) is present. Both CFA and SS are reactive to geopolymerization, which corresponds to the increase of compressive strength.

Preprints (www.preprints.org) | NOT PEER-REVIEWED | Posted: 23 November 2020 doi:10.20944/preprints202011.0580.v1

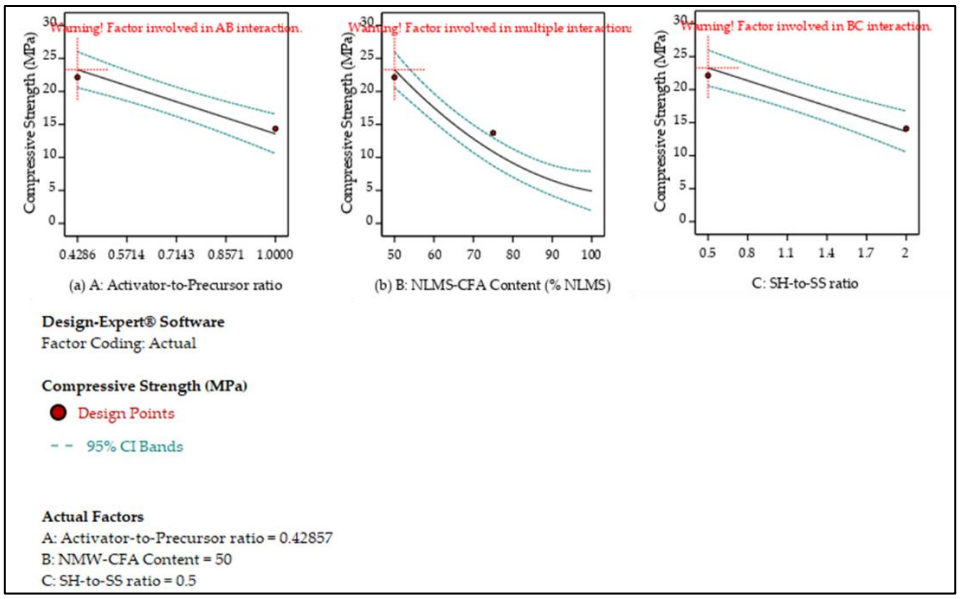

Figure 4. One-factor plot.

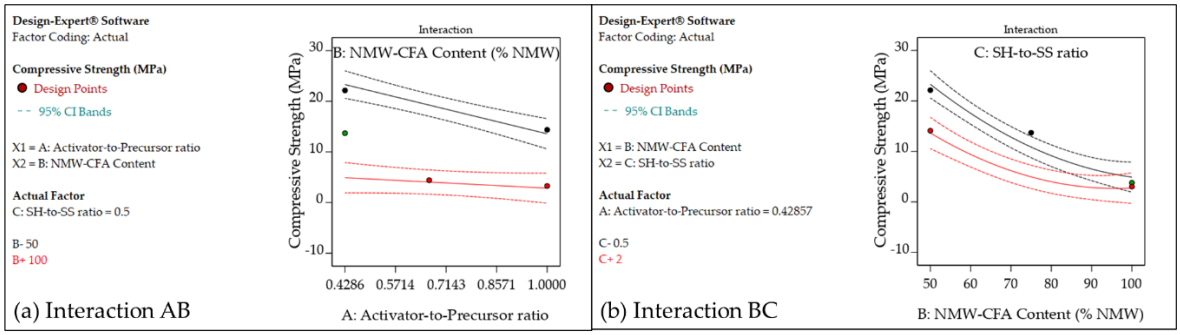

Figure 5. Interaction graph.

3.1.3. Regression Model

The regression result further explains the result of ANOVA. The resulting linear regression model in actual values is as follows:

$$Y = 86.337 - 30.408A - 1.310B - 11.408C + 0.268AB + 0.0996BC + 0.0052B^2$$

where:

$Y = Compressive\ strength, MPa$

$A = Activator - to - precursor\ ratio$

$B = NMW - CFA\ content, \%\ NMW$

$C = SH - to - SS\ ratio$

From the equation, it can be observed that factor B (%NMW) can significantly affect the compressive strength of the geopolymer as it is present in 4 out of 7 coefficients in the equation. It was further verified through a sensitivity analysis of factors (Table 8) when one factor is changed by 75%, 50%, and 25%, and the other two factors are fixed. For instance, in the "changed value by 75%" column, only factor A is changed from 0.43 to 0.75. The resulting calculated compressive strength is 17.9 MPa, with a percent change of -23.4%. Similarly, when factor B is changed, the compressive strength is calculated at 7.20 MPa (-69.2%). When factor C is changed, the resulting compressive strength is 20.2 MPa (-10.3%). Factor B shows the most significant change in compressive strength. Similarly, when each factor is changed by 50% and 25%, factor B has the highest percentage change when each factor is changed.

Preprints (www.preprints.org) | NOT PEER-REVIEWED | Posted: 23 November 2020 doi:10.20944/preprints202011.0580.v1

Table 8. Sensitivity analysis of factors.

Factor	Range	Low	High	changed value by 75%			changed value by 50%			changed value by 25%		
				Changed A	Changed B	Changed C	Changed A	Changed B	Changed C	Changed A	Changed B	Changed C
A	0.429 to 1	0.429	1	0.75	0.429	0.429	0.643	0.429	0.429	0.536	0.429	0.429
B	50 to 100	50	100	50	87.5	50	50	75	50	50	62.5	50
C	0.5 to 2	0.5	2	0.5	0.5	0.875	0.5	0.5	0.75	0.5	0.5	0.625
Y		23.3	0.833	17.9	7.20	20.9	19.7	10.9	21.7	21.5	16.3	22.5
% changes from low value				**-23.4%**	**-69.2%**	**-10.3%**	**-15.6%**	**-53.1%**	**-6.9%**	**-7.8%**	**-30.0%**	**-3.4%**

3.1.4. Response Surface Model (Optimization)

The numerical optimization tool of the Design Expert software was used to find the optimal point on the response surface to maximize the unconfined compressive strength of the synthesized geopolymer. The selected values were followed in the region where maximum strength can be seen, which from Figure 6, it can be observed that the maximum strength is approaching the minimum values of all the factors.

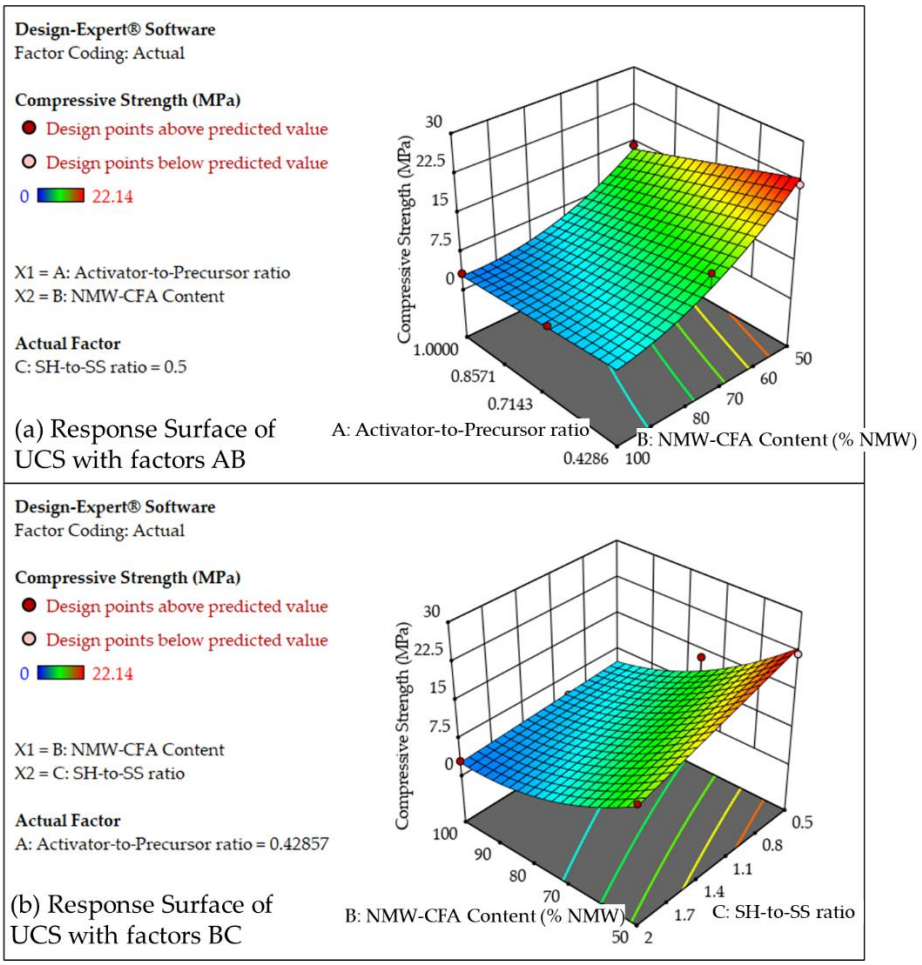

Figure 6. Response Surface of Unconfined Compressive Strength.

With a desirability of 1.0, the calculated optimized mix formulation is obtained with an activator-to-precursor ratio of 0.438, percent NMW of 50.1%, and an SH-to-SS ratio of 0.520. The predicted value is calculated at 22.9 MPa with a predicted R^2 equivalent of 0.890.

Preprints (www.preprints.org) | NOT PEER-REVIEWED | Posted: 23 November 2020 doi:10.20944/preprints202011.0580.v1

3.2. Confirmatory Run

Using the calculated optimized mix formulation obtained with an activator-to-precursor ratio of 0.438, percent NMW of 50.121%, and an SH-to-SS ratio of 0.520, a confirmatory run of the synthesized geopolymer was performed. The actual unconfined compressive strength of the confirmatory run was obtained to be 36.3 MPa with a deviation of -57.97% (Table 9.).

Table 9. Predicted and actual values of UCS of the confirmatory run.

A: Activator-to-Precursor ratio	B: NMW-CFA Content (% NMW)	C: SH-to-SS ratio	Predicted UCS MPa	Actual UCS MPa	% Deviation
0.438	50.1	0.520	22.9	36.3	-57.97%

The deviation of -57.97% could be attributed to the noise that was not measured during the experiment. Nonetheless, the result is in reasonable agreement with the predicted R^2 equivalent to 0.8902. The deviation may be attributed to the uncontrolled external factors, such as the type and strength of manual mixing of raw materials, the person who mixed the mixture, and the UCS equipment used for the optimized sample analyzed by a third party.

3.3. Morphological Properties of Synthesized Geopolymer

Figure 7 shows the different images of synthesized geopolymer with different NMW-CFA content. Synthesized geopolymer using 100% NMW has shown to have several voids and more unreacted NMW, which resulted to a lower compressive strength compared to a matrix with compact structure. The morphology of geopolymer with 75% NMW has cemented surfaces but with fewervoids and fewer unreacted NMW, which can be a factor of a higher compressive strength than the previous geopolymer. Geopolymer with 50% NMW has the most apparent or widest distribution of cemented surfaces among the geopolymers, which signifies a higher compressive strength. Although, there are some spherical shapes seen, which is unreacted coal fly ash. On the other hand, the optimized sample has a larger area of cemented surface, which explains its highest compressive strength for all the samples.

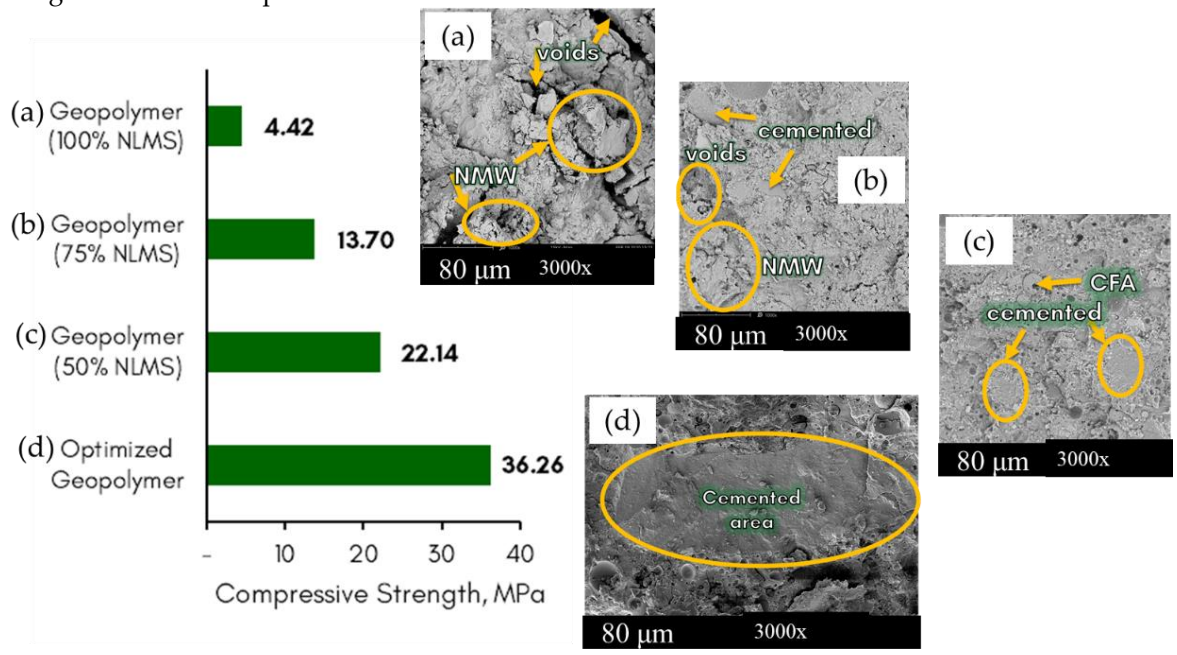

Figure 7. SEM Images of Synthesized Geopolymer at different precursor mix (1000x) with corresponding UCS.

3.4. Potential Engineering Application

Table 10 shows the unconfined compressive strength of the synthesized geopolymer (optimized, 50% NLMS, 75% NLMS, and 100% NLMS) and compared to several materials for a potential

Preprints (www.preprints.org) | NOT PEER-REVIEWED | Posted: 23 November 2020 doi:10.20944/preprints202011.0580.v1

application. Based on the standard unconfined compressive strengths, the synthesized geopolymers can have a potential application for pavers and building bricks, plain concrete for curbs and sidewalks, veneers, hollow bricks, masonry bricks, plain concrete for leveling, ceramic bricks, and load-bearing and non-load bearing masonry bricks. It also shows that even at a lower compressive strength of the geopolymer, it still has potential engineering applications.

Table 10. Comparison of unconfined compressive strength from the standard materials.

Material	Mixture	Application	UCS (MPa)	Source
Class A Concrete	OPC-sand mixture	Concrete structures and concrete pavements	20.7	DPWH and ASTM Standards
Class C Concrete	OPC-sand mixture	Pedestrian & Light Traffic Paver	20.7	DPWH and ASTM Standards
Class B Concrete	OPC-sand mixture	Plain concrete for structure (curbs, gutter, sidewalks)	16.5	DPWH and ASTM Standards
Class F Concrete	OPC-sand mixture	Plain concrete for leveling	11.8	DPWH and ASTM Standards
Grade S Concrete	OPC-sand mixture	Building bricks high strength and resistance	24.13	ASTM C55 Standard
Grade N Concrete	OPC-sand mixture	Building bricks medium strength and resistance	17.24	ASTM C55 Standard
C62 Grade Bricks	Clay or Shale	Building bricks	17.20	ASTM C 216 Standard
C902 Class Bricks	Clay or Shale	Pedestrian and Light Traffic Paving Brick	24.10	ASTM C 216 Standard
C126 Coring Bricks	Clay or Shale	Ceramic Glazed Facing Brick	10.3 to 17.2	ASTM C 216 Standard
Fired Clay Bricks	Clay	Load-bearing Masonry Bricks	5 to 10	Australian/New Zealand Standards
Fired Clay Bricks	Clay	Non-load bearing Masonry bricks	3 to 5	Australian/New Zealand Standards
Geopolymer	**Optimized sample**	**Pavers, Bricks**	**36.3±3.6**	This study, 2020
	50% NMW; 50% CFA	**Pavers**	**22.1±5.4**	
	75% NMW; 25% CFA	**Coring Bricks**	**13.7±2.9**	
	100% NMW	**Clay Bricks**	**4.42±0.3**	

4. Conclusions

This paper presents an experimental study to produce an optimized geopolymer material that yields the highest value of unconfined compressive strength from the mixture of nickel-laterite mine waste (NMW), coal fly ash (CFA), and an alkali activator with components of sodium hydroxide (SH) and sodium silicate (SS). The optimum formulation mix was found to have an activator-to-precursor ratio of 0.428, %NMW of 50.121%, and SH-to-SS ratio of 0.52, which produces a geopolymer with an average 28-day compressive strength of 36.26 MPa. This value is comparable to ordinary Portland cement for pedestrian pavers, light traffic pavers, plain concrete leveling, and building bricks. Other mix formulations with lower unconfined compressive strength like the 100% NMW with 4.42 MPa can also be used for fired clay bricks in masonry.

The result of SEM/EDX also showed that the optimum formulation has a cemented surface, resulting in a high unconfined compressive strength. The sample with low compressive strength was observed to have large voids in the microstructure, explaining its lower unconfined compressive strength.

Future work includes exploring the effect of the iron content of the NMW in the synthesis of the geopolymer. It is also recommended to explore the formulation mix of the synthesized geopolymer when the percentage of NMW is less than 50%. The curing duration of more than 28 days and its effect on the compressive strength can also be explored.

Author Contributions: Conceptualization, M.P..; methodology, A.L., A.T., and I.D.; validation, R.M., I.A., and M.P.; formal analysis, A.L., and A.T.; investigation, M.P.; resources, M.P.; data curation, A.L., and A.T.; writing—original draft preparation, A.L.; writing—review and editing, M.P., I.A., R.M., A.T., and I.D.; visualization, A.L., and I.D.; supervision, M.P., H.H., W.K., I.A.; and R.M.; project administration, A.T.; funding acquisition, M.P. All authors have read and agreed to the published version of the manuscript.

Funding: This research was funded by the Department of Science and Technology-Philippine Council for Industry, Energy and Emerging Technology Research and Development (Project No. 07132) under the implementing agency of the Center for Engineering and Sustainable Development Research, De La Salle University-Manila and the APC was funded by Department of Science and Technology-Engineering Research and Development for Technology.

Acknowledgments: Authors acknowledge the following organizations: Department of Transdisciplinary Science and Engineering of Tokyo Institute of Technology; iNano Research Facility, De La Salle University; Advanced Device and Materials Testing Laboratory; Office of the Vice-Chancellor for Research and Innovation, De La Salle University, Philippines; Ceramics Engineering, MSU-Iligan Institute of Technology, Philippines Agata Mining Ventures, Inc. (AMVI); and STEAG Power, Inc.

Conflicts of Interest: The authors declare no conflict of interest. The funders had no role in the design of the study; in the collection, analyses, or interpretation of data; in the writing of the manuscript, or in the decision to publish the results.

References

[1] M. S. Reddy, P. Dinakar, and B. H. Rao, "Mix design development of fly ash and ground granulated blast furnace slag based geopolymer concrete," *J. Build. Eng.*, vol. 20, pp. 712–722, 2018.

[2] S. V. Patankar, Ghugal Yuwaraj M., and S. S. Jamkar, "Mix Design of Fly Ash Based Geopolymer Concrete," *Adv. Struct. Eng. Mater. Vol. Three*, pp. 1619–2647, 2015.

[3] D. Kanesan, S. Ridha, and P. Rao, "Formulation of geopolymer cement using mixture of slag and class f fly ash for oil well cementing," *IOP Conf. Ser. Mater. Sci. Eng.*, vol. 201, no. 1, 2017.

[4] N. Li, C. Shi, Z. Zhang, H. Wang, and Y. Liu, "A review on mixture design methods for geopolymer concrete," *Compos. Part B Eng.*, vol. 178, no. April, p. 107490, 2019.

[5] H. K. Tchakouté, C. H. Rüscher, M. Hinsch, J. N. Y. Djobo, E. Kamseu, and C. Leonelli, "Utilization of sodium waterglass from sugar cane bagasse ash as a new alternative hardener for producing metakaolin-based geopolymer cement," *Chemie der Erde*, vol. 77, no. 2, pp. 257–266, 2017.

[6] M. W. Ferdous, O. Kayali, and A. Khennane, "A detailed procedure of mix design for fly ash based geopolymer concrete," *Proc. 4th Asia-Pacific Conf. FRP Struct. APFIS 2013*, no. December, pp. 11–13, 2013.

[7] A. Longos, A. A. Tigue, R. A. Malenab, I. J. Dollente, and M. A. Promentilla, "Mechanical and thermal activation of nickel-laterite mine waste as a precursor for geopolymer synthesis," *Results Eng.*, vol. 7, no. April, p. 100148, 2020.

[8] L. Zhang, S. Ahmari, and J. Zhang, "Synthesis and characterization of fly ash modified mine tailings-based geopolymers," *Constr. Build. Mater.*, vol. 25, no. 9, pp. 3773–3781, 2011.

[9] J. G. S. Van Jaarsveld, J. S. J. Van Deventer, and G. C. Lukey, "04/00191 The characterization of source materials in fly ash-based geopolymers," *Fuel Energy Abstr.*, vol. 45, no. 1, p. 23, 2004.

[10] B. Li, H. Wang, and Y. Wei, "The reduction of nickel from low-grade nickel laterite ore using a solid-state deoxidisation method," *Miner. Eng.*, vol. 24, no. 14, pp. 1556–1562, 2011.

[11] H. Liu, Q. Sun, B. Wang, P. Wang, and J. Zou, "Morphology and composition of microspheres in fly ash from the luohuang power plant, Chongqing, Southwestern China," *Minerals*, vol. 6, no. 2, 2016.

[12] C. Phetchuay, S. Horpibulsuk, A. Arulrajah, C. Suksiripattanapong, and A. Udomchai, "Strength development in soft marine clay stabilized by fly ash and calcium carbide residue based geopolymer," *Appl. Clay Sci.*, vol. 127–128, pp. 134–142, 2016.

[13] A. A. Aliabdo, A. E. M. Abd Elmoaty, and H. A. Salem, "Effect of water addition, plasticizer and alkaline solution constitution on fly ash based geopolymer concrete performance," *Constr. Build. Mater.*, vol. 121, pp. 694–703, 2016.

[14] M. A. B. Promentilla *et al.*, "Optimizing ternary-blended geopolymers with statistical multi-response surface analysis," *J. Chem. Inf. Model.*, vol. 53, no. 9, pp. 1689–1699, 2013.

[15] P. Pavithra, M. Srinivasula Reddy, P. Dinakar, B. Hanumantha Rao, B. K. Satpathy, and A. N. Mohanty, "A mix design procedure for geopolymer concrete with fly ash," *J. Clean. Prod.*, vol. 133, pp. 117–125, 2016.

[16] J. N. Yankwa Djobo, A. Elimbi, H. Kouamo Tchakouté, and S. Kumar, "Mechanical properties and durability of volcanic ash based geopolymer mortars," *Constr. Build. Mater.*, vol. 124, pp. 606–614, 2016.